A GIS Approach to Analysis of Deep-Seated Slope Stability in Complex Geology

Ivan Marchesini, Martin Mergili, Mauro Rossi, Michele Santangelo, Mauro Cardinali, Francesca Ardizzone, Federica Fiorucci, Barbara Schneider-Muntau, Wolfgang Fellin, and Fausto Guzzetti

Abstract

We demonstrate the computer model r.rotstab.layers to explore the possibilities of GIS for catchment-scale deep-seated slope stability modelling in complex geology. This model makes use of a modification of the three-dimensional sliding surface model proposed by Hovland and revised and extended by Xie and co-workers. It evaluates the slope stability for a large number of ellipsoidal random slip surfaces which may be truncated at the interfaces between geological layers. This results in a spatial overview of potentially unstable regions. After demonstrating the functionality of the model with an artificial cone-shaped terrain, we test r.rotstab.layers for the 10 km^2 Ripoli area in Umbria, central Italy. According to field observations in the Ripoli area, morpho-structural settings play a crucial role for deep-seated landslide distribution. We have prepared a model of the geological layers based on surface information on the strike and dip of each layer, and we use this model as input for r.rotstab.layers. We show that (1) considering the geological layers is essential for the outcome of deep-seated slope stability modelling, and (2) the seepage direction of the groundwater is a major source of uncertainty.

Keywords

Geological layers • Slip ellipsoid • Slope stability • Open source GIS

I. Marchesini • M. Santangelo • M. Cardinali • F. Ardizzone • F. Fiorucci • F. Guzzetti
CNR IRPI, Via Madonna Alta 126, 06128 Perugia, Italy
e-mail: ivan.marchesini@irpi.cnr.it; Michele.santangelo@irpi.cnr.it; mauro.cardinali@irpi.cnr.it; francesca.ardizzone@irpi.cnr.it; federica.fiorucci@irpi.cnr.it; fausto.guzzetti@irpi.cnr.it

M. Mergili (✉)
Institute of Applied Geology, BOKU University, Peter-Jordan-Straße 70, 1190 Vienna, Austria
e-mail: martin.mergili@boku.ac.at

M. Rossi
CNR IRPI, Via Madonna Alta 126, 06128 Perugia, Italy

Department of Earth Sciences, University of Perugia, Piazza dell'Universitá 1, 06100 Perugia, Italy
e-mail: mauro.rossi@irpi.cnr.it

B. Schneider-Muntau • W. Fellin
Unit of Geotechnical and Tunnel Engineering, University of Innsbruck, Technikerstrasse 13, 6020 Innsbruck, Austria
e-mail: barbara.schneider-muntau@uibk.ac.at; wolfgang.fellin@uibk.ac.at

Introduction

Simple deterministic slope stability models based on the assumption of an infinite slope with a planar failure plane parallel to the slope are commonly implemented in GIS environments (Van Westen et al. 2006). They are well suited for analyzing shallow slope stability. More complex models consider the three-dimensional geometry of possible slope failures and are therefore also suitable for the analysis of deep-seated slope stability (e.g., Bishop 1954; Janbu et al. 1956). Such models rely on complex neighbourhood relationships and their implementation in GIS environments is not trivial (attempts were made, e.g., by Xie et al. 2003, 2004a, b, 2006; Marchesini et al. 2009; and Jia et al. 2012). Mergili et al. (2014) have recently introduced the model r.rotstab in order to bridge the gap between the two approaches. They have found out that the model performance for deep-seated landslides may suffer from a

K. Sassa et al. (eds.), *Landslide Science for a Safer Geoenvironment*, Vol. 2,
DOI 10.1007/978-3-319-05050-8_75,

disregard of morpho-structural settings—in particular, the strike and dip of the geological layers—even though a clear statistical relationship with landslide occurrence was shown by Santangelo et al. (2014). In this article, we attempt to overcome this limitation of r.rotstab by extending the model with a tool—r.rotstab.layers—to include the strike and dip of the geological layers into the slope stability calculations. The objective of the work is to identify the capability of such an approach, as well as its limitations, and the most urgent needs for further research.

Methods

The Model r.rotstab

r.rotstab (Mergili et al. 2014) represents a GIS-based, three-dimensional slope stability model capable of dealing with both shallow and deep-seated slope failures. The model is developed as a C-based raster module within the GRASS GIS software (GRASS Development Team 2013). It makes use of a modification of the three-dimensional sliding surface model proposed by Hovland (1977) and revised and extended by Xie et al. (2003, 2004a, b, 2006). Compared to this model, a more advanced approach to compute the seepage forces is introduced, which is described in detail in Mergili et al. (2014). Given a Digital Elevation Model (DEM) and a set of thematic layers, the model evaluates the slope stability for a large number of randomly selected potential slip surfaces, ellipsoidal in shape. Randomization of the ellipsoid parameters is constrained by user-defined minima and maxima of the ellipsoid dimensions and position. Truncated ellipsoids can be used to model the presence of weak layers at defined depths—or defined regular or irregular surfaces—within the soil or the bedrock. Any single GIS raster cell may be intersected by multiple sliding surfaces, each associated with a computed safety factor. For each cell, the lowest value of the safety factor and the depth of the associated slip surface are stored. These pieces of information can be used to obtain a spatial overview of potentially unstable regions over an area of up to several square kilometres.

The Extended Model r.rotstab.layers

In r.rotstab, the geotechnical parameters required as input are defined on the basis of soil classes, discrete data units containing information on (i) cohesion c, (ii) angle of internal friction ϕ, (iii) dry specific weight γ_d and (iv) saturated water content Θ_s. r.rotstab further allows the definition of a limited number of layers for each soil class. Each ellipsoid is truncated at each layer bottom it intersects, and the safety factor is computed for the entire ellipsoid as well as for the truncated shapes. However, this design is not suitable for large amounts of layers in complex geological settings.

r.rotstab.layers is designed in order to overcome this limitation. Relying on input raster datasets representing the bottom of each geological layer, it can handle sets of up to 100 of such layers. The layer data is condensed into a text file which stores the depth of each relevant layer for each raster cell. The geotechnical parameters associated with each layer are required as tabular input. In contrast to r.rotstab, the information on the soil classes is provided by the layer data so that no additional horizontal soil classes have to be defined. Here, we present a preliminary version of the model.

Test with an Artificial Cone

Data

A regular cone with a slope of 30° is used to demonstrate the model performance in a controlled way. A set of regular and parallel geological layers with bedding planes at a constant dip of 30° is introduced, resulting in a varying orientation of the layers with respect to the cone surface (Fig. 1). A sequence of alternating 20 m thick strong ($c = 10$ kN/m^2, $\phi = 40°$) layers and 2 m thick weak ($c = 5$ kN/m^2, $\phi = 20°$) layers is defined, with the uppermost weak layer assumed at a depth of 10 m. In total, 54 layers are considered.

Taking an area of 1,000 × 1,000 m and a cell size of 5 m, r.rotstab.layers is run for 200,000 randomly centred ellipsoids with a length of 200 m, a width of 125 m and a depth of 20 m. In addition, two pre-defined ellipsoids (E1 and E2 in Fig. 2) are analysed in more detail.

Results and Discussion

Figure 1 shows the spatial variation of the safety factor yielded by r.rotstab.layers, assuming dry (a) and fully saturated (b) conditions. The side of the cone with bedding dipping in the direction of the slope clearly shows lower safety factors than the side with bedding dipping into the slope. This effect is enhanced for saturated material when considering layer-parallel seepage forces.

The results for two pre-defined ellipsoids—E1 with cataclinal (see Fig. 2a), E2 with anaclinal layering (see Fig. 2b)—are illustrated in terms of the forces acting along a longitudinal section through the centres of the ellipsoids. The shear resistance is positive in an upslope direction, shear forces and seepage forces are positive in a downslope direction. The shear resistance and the shear force are parallel to the local inclination of the slip surface. The seepage force

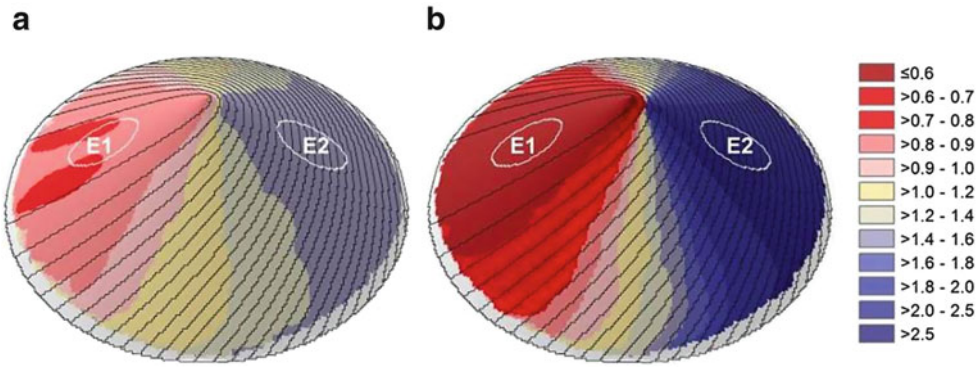

Fig. 1 Safety factors computed with r.rotstab.layers for a regular cone assuming (**a**) dry material, (**b**) saturated material with layer-parallel seepage. The black lines represent the traces of the weak layers, the ellipsoids E1 and E2 are analyzed in Fig. 2

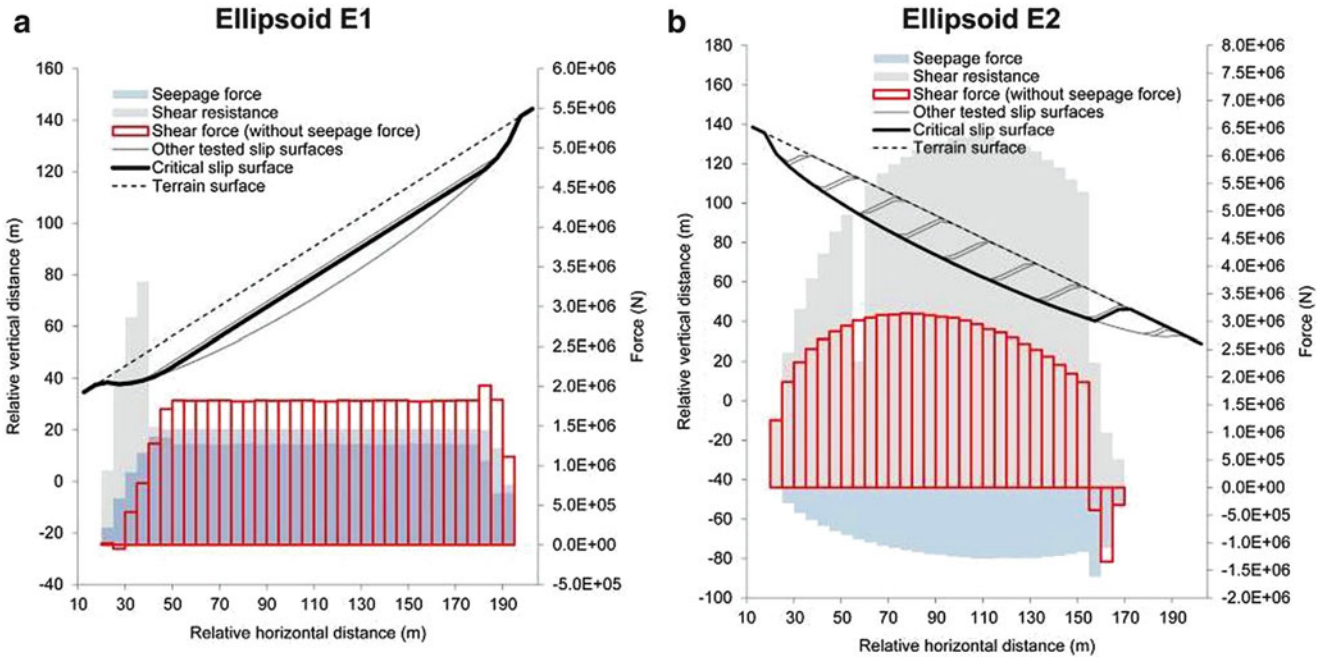

Fig. 2 Forces acting along the main axes of the ellipsoids E1 and E2 (see Fig. 1) for saturated conditions

acts in the direction of the seepage flow and the component parallel to the shear force is evaluated.

For the ellipsoid E1, the most critical slip surface (safety factor = 0.84 for dry conditions, 0.52 for fully saturated conditions) corresponds to the bottom of the only weak layer intersected by the ellipsoid bottom. The shear resistance is higher in the lower part of the ellipsoid, presenting a low inclination and high values of c and ϕ (slip surface within the strong layer). The shear resistance in the upper part of the ellipsoid is lower although high values of c and ϕ are applied, due to the steeper inclination and the lower weight. The patterns observed for the shear force and the seepage force reflect the balance between the inclination and the weight of the overlying saturated material and water, respectively.

The ellipsoid E2 intersects several weak layers of anaclinal setting (see Fig. 2b). Much higher safety factors (1.49 for dry conditions, 3.32 for saturated conditions) are observed than for E1, and higher safety factor are observed for saturated than for dry conditions. This is a consequence of (i) the high shear resistance over most of the tested slip surfaces, (ii) the negative shear force of the anaclinal-truncated surface and (iii) the negative seepage force (seepage into the slope as prescribed by the anaclinal orientation). Even though the effect of the weak layers on the shear resistance is obvious, in some places the spatial resolution does not allow identifying each single weak layer intersecting the ellipsoid bottom (see the single drop of the shear resistance in Fig. 2b).

Application to the Ripoli Area

Data

The Ripoli area is part of the Collazzone area (Umbria, central Italy) which has been intensively studied with regard to landslides in the past 15 years (Guzzetti et al. 2006; Ardizzone et al. 2007; Galli et al. 2008; Rossi et al. 2010; Fiorucci et al. 2011; Mergili et al. 2014). With an area of 9.7 km^2 (9.9 % of it affected by observed deep-seated landslides) the Ripoli area mainly consists of semi-consolidated clastic sediments. Particularly those with significant clay content are prone to landsliding (Fig. 3). The geotechnical parameters for each class exposed at the surface (Table 1) were determined by a combination of laboratory tests, a geotechnical data base for central Italy and back-calculations (Mergili et al. 2014). The bedding traces of the geological layers were mapped. Strike and dip of the traces were obtained at several places (Marchesini et al. 2013). From these pieces of information we generated the interpolated raster layers of bedding inclination and dip direction Santangelo et al. (2014), that were used to produce the TOBIA index map (Meentemeyer and Moody 2000) and the map of the dip direction relative to the slope (Fig. 3). By means of a GRASS GIS Python script and in particular of the Pygrass library (Zambelli et al. 2013), the elevation of the cells of the bedding surface corresponding to each stratigraphic limit is determined iteratively, starting from the stratigraphic limit outcrop and exploiting dip direction and inclination of the neighbouring cells. Altogether, the bedding planes of 67 layers—all of them >2 m thick—are used as input for r.rotstab.layers, each of them assigned to one of the six classes shown in Table 1. In addition we use a 10 m resolution DEM derived from a set of contour lines shown in the 1:10,000 topographic map. The model is run for three sets of assumptions: (i) no layering, with distribution of soil classes according to Fig. 3 and no truncation of the ellipsoid (original r.rotstab), (ii) layering, but seepage assumed in slope-parallel direction, (iii) layering with seepage in the dip direction of the layers. All of the assumptions are based on fully saturated material.

The random ellipsoids are constrained according to the dimensions of deep-seated landslides observed in the Collazzone area (length = 65–266 m, width = 55–291 m, depth = 5–20 m, Mergili et al. 2014). One million ellipsoids are tested during each model run.

Results and Discussion

The spatial distribution of the safety factor computed with the assumptions (a), (b) and (c) is illustrated in Fig. 4. The results are validated with the distribution of observed deep-seated landslides in the Ripoli area. As the ellipsoids have to be centred within the study area, the edges of the area are not fully covered by the computation process and are therefore not considered for the validation procedure. Table 2 summarizes the main indicators of the validation for each of the three model runs. Looking at Fig. 4 and Table 2, it is obvious that assumption (b) yields the most conservative results, compared to the other assumptions. The safety factor is <1 for 70.8 % of the Ripoli area, in contrast to 30.5 % (a) and 23.5 % (c). Whilst 83.5 % of all observed landslide raster cells are identified correctly with assumption (b), this is only the case for 30.4 % of all raster cells without observed landslides. The assumptions (a) and (c) yield reverse patterns. The total rate of true predictions is significantly lower for the outcome of assumption (b) than for the other assumptions (35.1 %, compared to 67.7 % and 73.0 %, respectively; see Table 2). Two aspects of the results deserve a closer discussion: (1) why does assumption (b) lead to more conservative results than the other assumptions? and (2) which of the assumptions is closest to reality, i.e., how to interpret the results with regard to landslide susceptibility mapping?

(1) With assumption (a), only the top layer is considered and assumed to be infinitely thick. For each raster cell, the probability that the ellipsoid surface intersects a susceptible material such as clay is much lower than if a layering approach with a possible truncation of the ellipsoid is adopted (assumptions b and c). With assumption (b), the seepage force always acts in the most unfavourable direction with respect to slope stability. Therefore the safety factors have a tendency to be lower than for assumption (c), where they can also act into the slope and therefore lead to an increased safety factor (see Figs. 1 and 2).

(2) First of all it seems clear that the assumptions (b) and (c) are superior to assumption (a) in capturing the complexity of the topic. Assumption (c) fails to reproduce two prominent landslides in the centre of the study area (see Fig. 4) which are well reproduced by assumption (b). Looking at Fig. 3, these two landslides are associated with orthoclinal layering, leading to seepage forces directed into the slope and therefore high safety factors with regard to assumption (c). However, the question of seepage direction is a complex one and requires more detailed work to be better understood and better implemented in this type of model.

Finally, the high false positive rate related to assumption (b) (see Table 2) is not necessarily purely a consequence of a poor understanding of the phenomenon and/or an insufficient parameterization. False positive raster cells may have been affected by earlier unmapped landslides or be susceptible to future landslides. In contrast, false negative predictions are certainly incorrect.

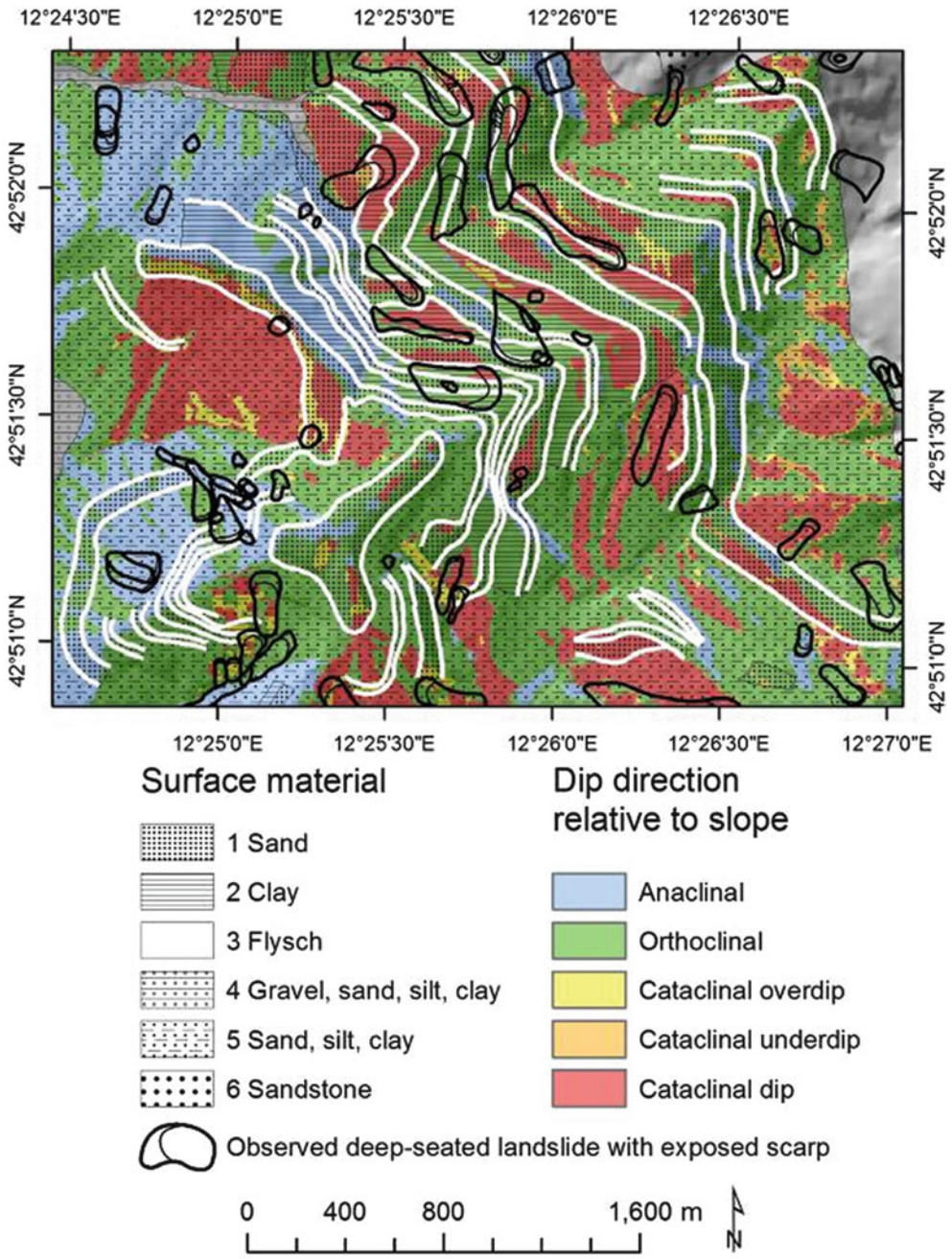

Fig. 3 Ripoli area. The white lines represent the bedding traces of the 67 geological layers considered. Each layer is assigned to one of the classes characterized in Table 1

Table 1 Material properties of the geological classes exposed in the Ripoli area: cohesion c (kN/m^2), angle of internal friction φ (degrees), dry specific weight γ_d (kN/m^3) and saturated water content Θ_s (vol. %)

ID type	γ_d	c	ϕ	Θ_s
1 Sand	19.0	4.0	38.0	40
2 Clay	15.5	8.3	18.1	25
3 Flysch	18.0	22.0	15.0	45
4 Gravel, sand, silt, clay	19.0	13.0	30.0	45
5 Sand, silt, clay	18.0	15.0	15.0	45
6 Sandstone	22.0	8.5	35.0	45

Conclusions

Employing a preliminary version of the new GIS-based three-dimensional slope stability model r.rotstab.layers, we have shown that the consideration of morpho-structural settings exerts a significant impact on the results of deep-seated slope stability computations. We conclude that the thickness, strike and dip of the geological layers have to be regarded for deep-seated landslide susceptibility mapping

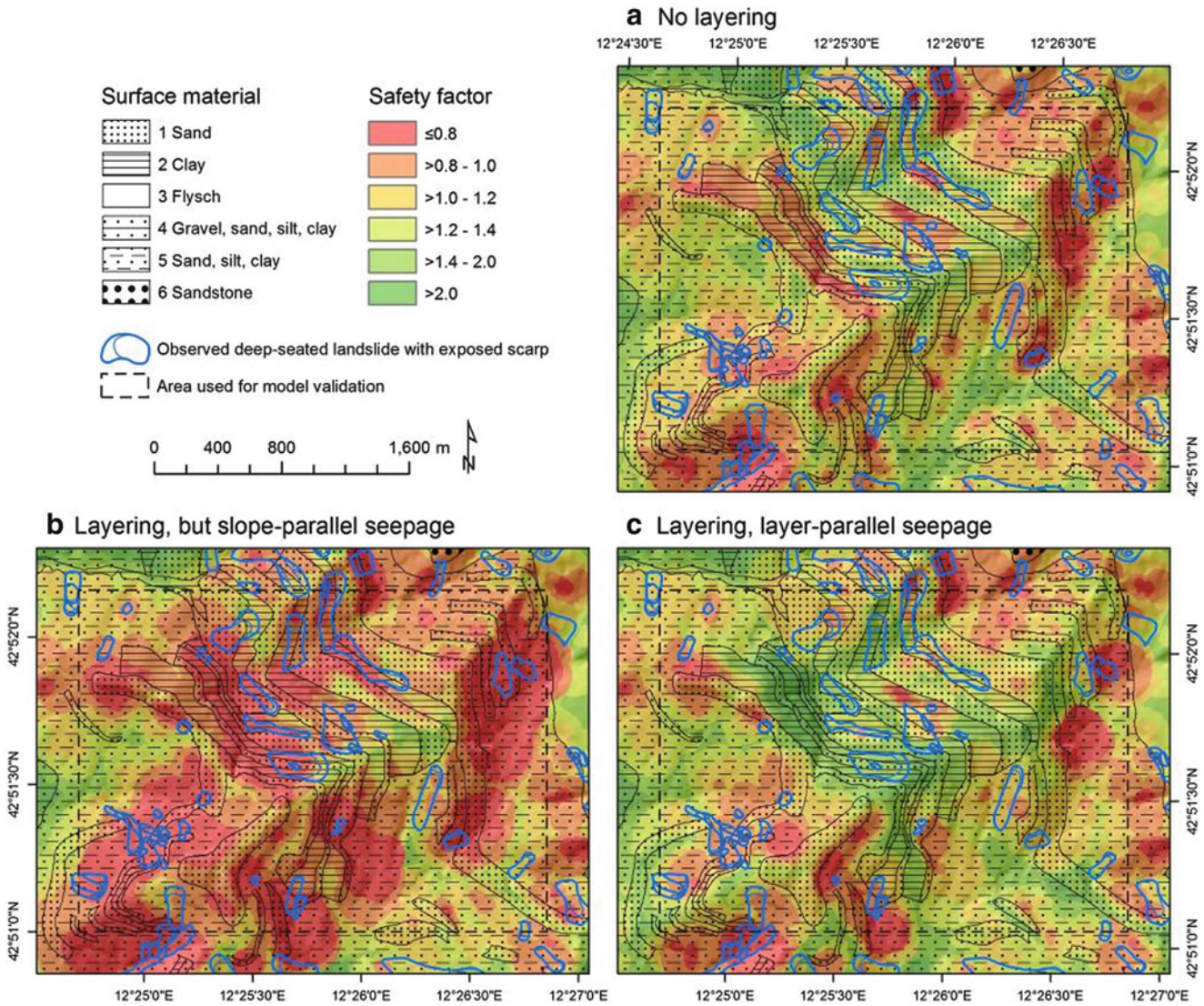

Fig. 4 Safety factors computed with three different assumptions of layering and seepage direction

Table 2 Model results for the Ripoli area

Predictions indicator	(a)	(b)	(c)
True negative—TN	64.2 %	27.7 %	70.3 %
False positive—FP	27.0 %	63.4 %	20.8 %
False negative—FN	5.3 %	1.5 %	6.2 %
True positive—TP	3.5 %	7.4 %	2.7 %
Rate of true non-landslide TN/(TN + FP)	70.4 %	30.4 %	77.1 %
Rate of true landslide TP/(FN + TP)	39.6 %	83.5 %	30.2 %
Total rate of landslide FP + TP	30.5 %	70.8 %	23.5 %
Total rate of true—TN + TP	67.7 %	35.1 %	73.0 %

(a) No layering, (b) layering, but slope-parallel seepage, (c) layering with seepage in dip direction of layers

efforts. Further, we have demonstrated that the seepage direction strongly influences the safety factor of saturated materials. We therefore recommend more research towards a detailed understanding of the—sometimes complex—seepage patterns in different types and assemblages of regolith.

Acknowledgments Special thanks go to Matthias Benedikt, Stefan Fugger, Sebastian Matz and Stefan Tilg. The work was partially supported by the Italian National Department for Civil Protection, and the Regione dell'Umbria under the contract POR-FESR Umbria 2007–2013.

References

Ardizzone F, Cardinali M, Galli M, Guzzetti F, Reichenbach P (2007) Identification and mapping of recent rainfall-induced landslides using elevation data collected by airborne Lidar. Nat Hazards Earth Syst Sci 7:637–650

Bishop AW (1954) The use of the slip circle in the stability analysis of slopes. Geotechnique 5(1):7–17

Fiorucci F, Cardinali M, Carlà R, Rossi M, Mondini AC, Santurri L, Ardizzone F, Guzzetti F (2011) Seasonal landslides mapping and estimation of landslide mobilization rates using aerial and satellite images. Geomorphology 129(1–2):59–70

Galli M, Ardizzone F, Cardinali M, Guzzetti F, Reichenbach P (2008) Comparing landslide inventory maps. Geomorphology 94:268–289

Guzzetti F, Galli M, Reichenbach P, Ardizzone F, Cardinali M (2006) Landslide hazard assessment in the Collazzone area, Umbria, Central Italy. Nat Hazards Earth Syst Sci 6:115–131

GRASS Development Team (2013) GRASS GIS. The world's leading Free GIS software. Open source geospatial foundation project. URL: http://grass.osgeo.org. Last accessed August 1, 2013

Hovland HJ (1977) Three-dimensional slope stability analysis method. J Geotech Eng Div ASCE 103(GT9):971–986

Janbu N, Bjerrum L, Kjaernsli B (1956) Soil mechanics applied to some engineering problems. Publication 16, Norwegian Geotechnical Institute, Oslo

Jia N, Mitani Y, Xie M, Djamaluddin I (2012) Shallow landslide hazard assessment using a three-dimensional deterministic model in a mountainous area. Comput Geotech 45:1–10

Marchesini I, Cencetti C, De Rosa P (2009) A preliminary method for the evaluation of the landslides volume at a regional scale. Geoinformatica 13:277–289

Marchesini I, Santangelo M, Fiorucci F, Cardinali M, Rossi M, Guzzetti F (2013) A GIS method for obtaining geologic bedding attitude. In: Margottini C, Canuti P, Sassa K (eds) Landslide science and practice. Springer, Berlin, pp 243–247

Meentemeyer RK, Moody A (2000) Automated mapping of conformity between topographic and geological surfaces. Comput Geosci 26:815–829

Mergili M, Marchesini I, Rossi M, Guzzetti F, Fellin W (2014) Spatially distributed three-dimensional slope stability modelling in a raster GIS. Geomorphology 206:178–195

Rossi M, Guzzetti F, Reichenbach P, Mondini AC, Peruccacci S (2010) Optimal landslide susceptibility zonation based on multiple forecasts. Geomorphology 114:129–142

Santangelo M, Marchesini I, Cardinali M, Fiorucci F, Rossi M, Bucci F, Guzzetti F (2014) A method for the assessment of the influence of bedding on landslide abundance and types. Landslides (Accepted)

Van Westen CJ, Van Asch TWJ, Soeters R (2006) Landslide hazard and risk zonation – why is it still so difficult? Bull Eng Geol Environ 65:167–184

Xie M, Esaki T, Zhou G, Mitani Y (2003) Three-dimensional stability evaluation of landslides and a sliding process simulation using a new geographic information systems component. Environ Geol 43:503–512

Xie M, Esaki T, Cai M (2004a) A GIS-based method for locating the critical 3D slip surface in a slope. Comput Geotech 31:267–277

Xie M, Esaki T, Zhou G (2004b) GIS-based probabilistic mapping of landslide hazard using a three-dimensional deterministic model. Nat Hazards 33:265–282

Xie M, Esaki T, Qiu C, Wang C (2006) Geographical information system-based computational implementation and application of spatial three-dimensional slope stability analysis. Comput Geotech 33:260–274

Zambelli P, Gebbert S, Ciolli M (2013) Pygrass: an object oriented python Application Programming Interface (API) for Geographic Resources Analysis Support System (GRASS) Geographic Information System (GIS). ISPRS Int J Geo-Inform 2(1):201–219